*Manuscript
Click here to view linked References

PEGylated carbon black as lubricant nanoadditive with enhanced dispersion stability and tribological performance

Virginia Ruiz[a,*], Luis Yate[b], Judith Langer[b], Ivet Kosta[a], Hans J. Grande[a], Ramón Tena-Zaera[a]

[a] CIDETEC, Paseo Miramón 191, E-20014 Donostia-San Sebastián, Spain.

[b] CIC biomaGUNE, Paseo Miramón 192, E-20014 Donostia-San Sebastián, Spain.

[*]Corresponding author. E-mail: vruiz@cidetec.es

Abstract

Poly(ethylene glycol) (PEG) chains were covalently grafted onto carbon black (CB) using a PEG-terminated trimethoxysilane, yielding PEGylated CB additives (CB-SiPEG) with different SiPEG contents. Unlike pristine CB, CB-SiPEG was readily dispersed in PEG200 base oil, with CB-SiPEG hydrodynamic particle sizes being considerably smaller than those of pristine CB. At optimal SiPEG content, friction coefficient and specific wear rate in ball-on-disk tribometer tests were reduced by 35% and 67% respectively, with 1% wt. CB-SiPEG compared to PEG200 alone. In contrast, pristine CB, alone or with unbound SiPEG, did not show friction-reducing or antiwear capacity. Disk analysis supports CB-SiPEG surface deposition forming a protective tribofilm. Hydrodynamic particle size and lubricating performance of CB-SiPEG/PEG200 blends were preserved after 6 months, indicating high dispersion stability.

Keywords: Carbon black, PEGylation, lubricant nanoadditives, high dispersibility.

1. Introduction

Numerous mechanical systems require lubricants to decrease the friction and wear of contacting surfaces hence reducing energy consumption. Therefore, there is a constant search for better lubricating fluids. In this regard, poly(alkyl ether)s like poly(ethylene glycol) (PEG) are commonly used synthetic base oils because they are eco-friendly, degradable and have shown high-performance lubricating performance for applications in gear oils, compressor lubricants, brake, hydraulic and metal working fluids, among others [1]. PEG is also used for tribological applications in the biomedical field to reduce friction and wear in knee joints [2]. However, its applications have been limited because conventional lubricant additives for mineral oils are not always effective for polar base oils such as ethers due to their poor compatibility [3]. Therefore, there has been intensive research focusing on new antiwear and friction-reducing additives suitable for polar base oils such as PEG [4-8]. Among them, ionic liquids have attracted considerable attention as lubricant additives for PEG [4]. Alternatively, a number of carbon nanomaterials have been reported as friction-reducing and antiwear solid additives for PEG with higher corrosion resistance than ionic liquids, including carbon dots [5], nanodiamonds [6], reduced graphene oxide [7] and carbon quantum dots/graphene oxide hybrid nanomaterials [8]. Although some nanomaterial-based additives exhibit high performance and attractive application prospects, the main drawback is the poor dispersibility and stability of carbon nanomaterials in PEG. This has probably hindered the use of more economic and abundant carbon nanomaterials with well-established lubricating properties such as graphite and carbon black nanoparticles, as friction-reducing and antiwear solid additives in polar base oils like PEG [9,10].

In fact, carbon black (CB) and activated carbons have long been used as solid lubricants [11,12] due to a better tribological performance compared to other carbon-based nanoadditives such as nanotubes or nanofibers dispersed in mineral oils [13,14]. Thus, CB has attracted considerable industrial interest as indicated by the number of patents of different

lubricating oils and greases comprising CB as friction-reducing additive [15-17]. Moreover, the tribological behavior and wear induced by CB in various oils has been investigated to simulate the effect of soot contamination in diesel engine oils due to incomplete combustion of hydrocarbons [18-21]. However, as stated already, the poor dispersibility of carbon powders such as CB in different oils makes the use of dispersants or surfactants indispensable. Typical dispersants for CB in mineral oils and greases include polybutenyl succinic acid imide and amide, benzylamine, succinic acid ester derivatives, polyoxyalkylene glycol derivatives, phosphate esters and alkyl-aryl-sulfonates [14-17]. Among them, polyoxyethylene (POE) derivatives (alcohols, esters, ethers or mercaptans) represent a class of non-ionic surfactants commonly used to disperse solid particles in polar media [22,23]. Some specific POE derivatives like polysorbates (POE sorbitan esterified with fatty acids) are emulsifiers in the pharmaceutical and food industry that have even been proposed as biocompatible dispersing agents for CB in blood plasma, cell culture media or physiological solutions for biological applications [24].

As an alternative to the use of dispersants, surface treatment or chemical modification of CB is a common strategy to tune CB particle wettability according to the dispersing media. Thus, surface modification of intrinsically hydrophobic CB particles with a number of functional groups has been proposed to increase surface wettability and hence stability in aqueous media, namely: carboxylic groups [25], nitrogen-containing groups such amine and pyridine-N-oxide moieties [26] or polymers such as polyvinyl alcohol [27]. Polymer chains were also covalently grafted on CB particles to improve dispersion in rubbers or resins [28, 29].

Inspired by the excellent dispersing properties and biocompatibility of POE derivatives, we report here the covalent functionalization of CB with PEG as a strategy to produce PEGylated CB, a lubricant additive highly dispersible in PEG base oil. To the best of our knowledge, PEGylated CB has not been investigated so far as friction modifier additive in lubricants even though PEG-treated CB has been proposed as conductive additive for polymer compounds

with enhanced rheological, mechanical and electrical properties [30]. Indeed, the use of free (non-bonded) PEG as CB dispersant is a rather common strategy in the polymer and rubber industry to promote CB compatibility with elastomer matrices [31-33]. In this paper, we have grafted PEG covalently on CB by silanization of hydroxylated CB with a hydrophilic trimethoxysilane with polar POE substitution (PEGylated), specifically 3-[methoxy (polyethyleneoxy)$_{6-9}$ propyl]trimethoxysilane (SiPEG). Unlike pristine CB, we will show that the resulting PEGylated CB (CB-SiPEG) can be readily dispersed in PEG200 (Mw = 200) base oil and the PEG200 blends with CB-SiPEG additive are stable for months. The tribological performance of a series of CB-SiPEG additives with different SiPEG grafting ratios in PEG200 has been assessed by a ball-on-disk tribometer using 100Cr6 steel ball and disk. At the optimal SiPEG grafting content, 35% and 67% reduction in friction coefficient and wear rate respectively were achieved with CB-SiPEG as additive in PEG200 base oil.

2. Materials and methods

2.1. Materials

Starting materials were purchased from the following commercial suppliers: Vulcan® XC-72 carbon black from Cabot Corporation, 3-[methoxy(polyethyleneoxy)$_{6-9}$ propyl]trimethoxysilane (90%) from abcr, nitric acid (60%), PEG200 (Mw = 200) and ethanol (96 %) from Sigma Aldrich. The density and dynamic viscosity of PEG200 at 25ºC are 1.124 g mL^{-1} and 51 mPa s, respectively. All chemicals were of analytical grade and used without further purification. Aqueous solutions were prepared with ultrapure water of Synthesis A10 from Millipore (18Ω.cm) (Massachusetts, USA).

2.2. Synthesis of PEGylated CB

In a first step, CB was subject to oxidative treatment to obtain a hydroxylated powder (CB-ox) with abundant hydroxyl surface groups (Figure 1). In a typical procedure, CB (2g) was dispersed in 6M nitric acid (250 mL) in an ultrasonic bath (1 h) and refluxed at 150ºC for 24h.

After cooling to room temperature, the suspension was centrifuged (3500 rpm) for 30 min to obtain CB-ox as sediment. The sediment was washed with ultrapure water followed by centrifugation three times and subsequently dried under vacuum. Next, CB-ox silanization was carried out by dispersing CB-ox (0.4 g) in a 1:1 mixture of ethanol and ultrapure water (100 mL) and adding different volumes of SiPEG (0.1-1 mL) to yield CB-SiPEG with different SiPEG grafting ratios. The mixture was heated with vigorous stirring in a silicon bath at 50ºC for 24h. After cooling to room temperature, the suspension was centrifuged (3500 rpm) for 2h to separate unreacted CB-ox as sediment and CB-SiPEG as supernatant. Ethanol was evaporated from the supernatant at 60ºC and CB-SiPEG was purified by in a dialysis bag (retained molecular weight: 3500 Da) for 1 day to remove unreacted SiPEG. The solution was finally freeze dried to obtain purified CB-SiPEG.

2.3. Material characterization

Additives and disk surfaces were examined by field-emission scanning electron microscopy (FE-SEM) and energy dispersive X-ray spectroscopy (EDS) in a Zeiss Ultra plus FE-SEM. FTIR spectra of additives were recorded at room temperature using a Jasco 4100LE spectrophotometer with 4 cm^{-1} resolution in a wavenumber range from 4000 to 400 cm^{-1}. Thermogravimetric analysis (TGA) of the additives was performed with a TGA Q500 (TA instruments) at a heating rate of 10 °C min^{-1} under air atmosphere. X-ray diffraction patterns of the samples were recorded between 10 and 60° (2θ) with 3s/0.02º step size on a Bruker D8 Discover diffractometer with a Cu-Kα source (λ = 0.154 nm) and equipped with a LynxEye PSD detector. XPS experiments were performed in a SPECS Sage HR 100 spectrometer with a non-monochromatic X-ray source (Magnesium Kα line of 1253.6 eV energy and a power applied of 250 W) and calibrated using the $3d_{5/2}$ line of Ag with a full width at half maximum (FWHM) of 1.1 eV. The particle size distribution of additive dispersions in PEG200 was measured by dynamic light scattering (DLS) using a Malvern Instruments Zetasizer Nano ZS at 25ºC.

Dynamic viscosity of PEG200 and CB-SiPEG/PEG200 blends at 25ºC was measured in a stress controlled rheometer (TA instruments, AR 2000ex) with a stainless steel cone-plate geometry (cone angle 2º, diameter 40 mm with a gap size of 57 µm) by performing continuous flow ramp from shear rates of 20 to 100 s^{-1}.

2.4. Tribological characterization

For tribology tests CB-SiPEG was dispersed in PEG200 by ultrasonication (15 min). The tribological properties of CB-SiPEG dispersions in PEG200 were analyzed by measuring friction using a ball-on-disk tribometer (CSM Instruments, Switzerland). A 100Cr6 steel ball (6 mm diameter, Anton Paar) was used to slide against a lubricated 100Cr6 steel disk polished to mirror finish (28 mm diameter and 3.5 mm thick, Aceros IMS) under the following conditions: 4 cm s^{-1} sliding speed, 10N normal load, 1h test duration, a temperature of 25ºC and a wear track radius of 2 mm. Given the relevance of soot-induced wear in engine oils, the testing conditions were selected in order to achieve measurable wear volumes on the disks to compare wear rate of different lubricant formulations. The hardness of ball and disk was 60-66 HRC. The surface roughness (Ra) of the balls was < 32 nm (according to supplier specifications). The average surface roughness (Ra) of the disks was 83 ± 21 nm (measured with a 3D optical confocal microscope in 10 disks along 1.25 mm length profiles from 6 different regions in each disk). The wear tracks on the disks were examined by optical microscopy (Leica Microsystems DM4000M) and a 3D optical surface metrology system combining confocal microscopy and interferometry (Leica Microsystems DCM 3D). The wear track volume was calculated from the average area of 2D profiles extracted from the 3D images in four separate sections of the circular track. Disk surface was also investigated by Raman spectroscopy in a confocal Raman microscope WITec 300R in 180º back-scattering configuration using a fibre-coupled 532 nm laser as excitation source with power of 15 mW focused through a 100 x objective (numerical aperture = 0.9). Back-scattered wavelengths

were measured with 50 ms integration time and analysed with 600 mm focal length, lens-based spectrometer equipped with 300 l/mm grating and back-illuminated CCD.

3. Results and discussion

3.1. Synthesis and characterization of PEGylated CB

As described in detail in the experimental section, CB was first oxidized in nitric acid to introduce surface oxygen groups to react further with SiPEG (Figure 1). Then, silanization of CB-ox was carried out with five different CB-ox:SiPEG ratios (1:0.25, 1:0.5, 1:0.75, 1:1 and 1:2.5) to produce CB-SiPEG with different SiPEG grafting content. Successful grafting of SiPEG on CB-ox was confirmed by several techniques such as FTIR transmission spectroscopy, TGA, XRD and XPS (Figure 2).

FTIR transmission spectra of pristine CB, oxidized CB (CB-ox) and PEGylated CB (CB-SiPEG) obtained by silanization with different CB-ox:SiPEG ratios are compared in Figure 2A. The FTIR spectrum of pristine CB is featureless and upon oxidation, new bands emerge in the spectrum of CB-ox: a broad absorption band at ~3500 cm^{-1} that can be assigned to the O-H stretching mode of hydroxyl groups and a band at 1728 cm^{-1} due to the C=O stretching vibration, that together with the band at about 1630 cm^{-1} due to the O-H deformation vibration in carboxyl groups, confirm the presence of carboxylic acid groups in CB-ox [34].

Upon silanization of CB-ox with different SiPEG grafting ratios, a number of new bands characteristic of SiPEG (spectrum c) are visible in the spectra of CB-SiPEG samples (spectra d-h). The intense band centered at 2939 and 2864 cm^{-1} can be assigned to the asymmetric and symmetric C-H stretching vibrations while bands at 1349 and 1457 cm^{-1} are related to C-H bending vibrations in -CH_2- groups. The bands in the range of 1084-1290 cm^{-1} correspond to C-O-C stretching vibrations from the grafted PEG chains. The characteristic peaks of the silane group can also be observed in CB-SiPEG at 784 and 820 cm^{-1} related to Si-C stretching vibrations and in the range of 925–1195 cm^{-1} due to Si-O stretching vibrations from the

methoxy (Si-O-CH_3) groups and siloxane (Si-O-Si) crosslinks. In general, the intensity of bands related to vibrations from bonds in the SiPEG chain increase in CB-SiPEG samples with the amount of SiPEG used in the silanization step (from sample d to h), pointing to a higher SiPEG grafting content. Moreover, the intensity of the bands corresponding to O-H stretching vibrations also increase with SiPEG grafting content in CB-SiPEG samples and can be ascribed to terminal hydroxyl groups in the grafted SiPEG chains after hydrolysis of the terminal methoxy group. Interestingly, the intensity of the peak at 1195 cm^{-1} related to the Si-O-C rocking vibration in SiPEG [35] does not decrease in CB-SiPEG samples and the relative intensity of this band to that at 2864 cm^{-1} due to C-H vibrations is similar in unreacted SiPEG and CB-SiPEG samples, supporting the covalent grafting of SiPEG to CB-ox. That is, SiPEG grafting on CB (i.e. formation of new Si-O-C bonds) balances the intensity decrease of the Si-O-C rocking vibration as a result of hydrolysis of the terminal methoxy groups in SiPEG. Conversely, the ratio of these two bands (Si-O-C to C-H) has been reported to decrease compared to that in unreacted SiPEG when SiPEG grafting occurs onto non-carbon atoms such as boron [36] due to formation of Si-O-B bonds and consequent lower amount of Si-O-C bonds in PEGylated BN nanomaterials than in unreacted SiPEG.

Thermogravimetric analysis (TGA) was also used to corroborate successful grafting of SiPEG and to determine the SiPEG grafting content in the different CB-SiPEG samples from the mass loss attributable to the decomposition of grafted SiPEG. Figure 2B shows representative TGA curves under air atmosphere of pristine, CB-ox and CB-SiPEG obtained with different CB-ox:SiPEG ratios. Derivative TGA of the samples are shown in supporting information, Figure S1. While thermal degradation in pristine CB starts at 540ºC, CB-ox displays a clear weight loss (10%) in the range of 100- 400ºC corresponding to elimination of hydroxyl and carboxylic surface groups. In SiPEG two weight losses are observed, one in the range of 150-300ºC related to decomposition of the trimethoxysilane group and a second one between 320 and 450ºC due to degradation of PEG chains [36]. In turn, PEGylated CB samples display

three degradation stages, the two first ones (better resolved in Figure S1) in the range of 150-450ºC corresponding to decomposition of grafted SiPEG chains and the third one between 450 and 660ºC related to the carbon core. The SiPEG grafting ratio (wt% of grafted SiPEG to initial carbon) for the different CB-SiPEG samples was determined from the weight loss of the two first degradation stages, ranging from 49 to 81% (Table 1). From now on, PEGylated CB samples will be abbreviated as CB-SiPEGx where x corresponds to the SiPEG grafting ratio determined from TGA.

PEGylated CB samples were further examined by XRD (Figure 2C). Pristine CB exhibits a diffraction peak located at $2\theta = 24.5°$ from the (002) disordered graphitic plane that indicates the coke-like structure of CB with disordered carbonaceous interlayers [37]. In addition, the lower intensity of the (100) peak at 43º associated with crystalline carbon [38], highlights the poor crystallinity of CB. Upon oxidation, a slight shift of the (002) peak to higher angles (24.9º) was noted for CB-ox, indicating that the interplanar distance between graphitic planes decreased as a result of oxidation. This effect has been previously observed for activated carbons treated with different oxidizing agents and has been ascribed to interactions between functional groups and re-arrangements to minimize interatomic repulsions induced by certain oxygen surface groups [34]. On the contrary, the (002) diffraction peak of CB is shifted to smaller angles in CB-SiPEG samples and the magnitude of the shift increases with SiPEG grafting ratio, ranging from 23.5º to 21.1º for the lowest and highest SiPEG content, respectively (Figure 2C and Table 1). This shift indicates a larger interlayer spacing of (002) plane in PEGylated CB caused by intercalated PEG chains, as observed in other polymer-grafted carbon nanomaterials [39]. Moreover, the intensity of the (100) peak decreases with increasing SiPEG grafting ratio in CB-SiPEG samples, revealing a lower crystallinity of the functionalized CB as a result of the disorder induced by SiPEG chains. In fact, in order to unambiguously prove that changes in XRD patterns of CB-SiPEG samples arise from grafted SiPEG chains, the XRD spectrum of a mixture containing CB and free SiPEG in excess (1:

100) was measured (supporting information, Figure S2). In this case, a negligible shift of the (002) diffraction peak was noted (24.2º) compared to those for CB-SiPEG samples (23.5º to 21.1º), suggesting that interlayer spacing is not largely affected by the presence of unbound SiPEG. Furthermore, the intensity of the (100) diffraction peak of the CB and free SiPEG mixture remains unchanged, also indicating that the crystallinity of pristine CB is not altered by unbound SiPEG.

The chemical composition of the different CB samples was also investigated by XPS. Survey spectra of CB, CB-ox and representative PEGylated CB samples are compared in Figure 2D, together with the corresponding atomic percentage contents for each element. Detailed deconvolution of C1s, O1s and Si2p XPS spectra for CB, CB-ox and PEGylated CB samples with the lowest and highest SiPEG grafting ratios are shown in supporting information, Figure S3. In general terms, XPS analysis further supports the assignment of functional groups from FTIR spectra and quantitative estimation of SiPEG grafting content from TGA. Upon oxidation of CB, oxygen content increases to 14.1% at. in the CB-ox sample, whose main components in C 1s and O 1s spectra correspond to C-C, C=O and C-O bonds (Figure S3B and C). XPS also corroborates successful silanization of CB-ox with SiPEG as the Si 2s and Si 2p peaks at 153.5 and 102.4 eV respectively, from Si-O and Si-C bonds, were clearly resolved in CB-SiPEG samples (spectra d-h in Figure 2D). In agreement with TGA estimation of SiPEG grafting ratios, Si atomic content increased in PEGylated CB from 2.2% to 2.8% for CB-SiPEG49 to CB-SiPEG80 samples. Moreover, there is an increasing trend in oxygen content (from 19.8% to 29.5%) with SiPEG grafting ratio in PEGylated CB samples. Comparing deconvoluted C 1s spectra of samples with the lowest and highest SiPEG contents (Figure S3D and G) we can see a remarkable increase in the relative intensity of the C-O bond component (at 286.4 eV) with respect to that of the C-C bond (at 284.8 eV) with increasing SiPEG grafting ratio. Thus, the C-O/C-C bonds ratio estimated from the C 1s spectra

components (Table S1) increase from 0.66 in CB-SiPEG49 to 5.40 in CB-SiPEG80, providing evidence of the formation of covalent C-O bonds between CB and SiPEG.

Upon PEGylation, CB loses its characteristic powder-like texture and becomes stickier with increasing SiPEG grafting content (insets of Figure 3), resulting in a slurry-like semifluid material at the highest SiPEG content (80% wt.). As discussed in next section, the semifluid nature of CB-SiPEG allows better dispersion of the PEGylated additives in PEG200 lube oil. FESEM micrographs reveal large size closely-packed agglomerates (i.e. constituted by nanograins of ~ 50 nm size, named hereafter primary nanoparticles) in pristine CB powder (Figure 3A, marked with arrows) whereas additional material around the CB particles (i.e. creating a matrix-like structure) can be detected in CB-SiPEG samples (Figure 3B and C, marked with arrows). As the SiPEG content increases, it becomes hard to distinguish between the CB particles and PEG matrix due to the higher density of the hybrid material.

3.2. Lubrication performance of PEG blends with PEGylated CB additives

As opposed to pristine CB, PEGylated CB additives were readily dispersed in polar PEG200 base oil without ultrasonication. However, all blends were sonicated for 15 minutes to ensure good homogeneity and particle dispersion for tribology characterization. Figure 4 shows representative friction coefficient measurements for 100Cr6 steel disks lubricated with neat PEG200 and 1% wt. dispersions of different additives in PEG200: pristine CB, SiPEG, CB-SiPEG49 and a mixture of CB and free SiPEG at a 1:1 ratio. Steady-state friction coefficient values for each blend are summarized in Table 1.

As can be seen, only the PEGylated CB additive reduces considerably the friction coefficient of PEG200 base oil (~ 0.115) by 29%, whereas each of the individual components (pristine CB and unbound SiPEG) as well as their mixture at the same concentration exhibit roughly the same tribological performance as neat PEG200. The poor friction-reducing properties of pristine CB (both alone and in presence of unbound SiPEG) can be related to their low dispersibility in polar PEG200 oil, as illustrated in photographs of the different blends in

Figure 4. In both blends of PEG200 and pristine CB, large agglomerates are visible by naked eye whereas CB-SiPEG forms very homogeneous dispersions with no visible sediment/agglomeration. Likewise, Hu et al. only noticed improvement in friction coefficient with CB in a base oil (150SN) when the additive was well dispersed by adding the dispersant polyisobutylene succinimide [19].

The excellent dispersion of PEGylated CB additives was corroborated by measuring particle size distributions in PEG200 by dynamic light scattering (supporting information, Figure S4). The average hydrodynamic sizes for different additives at 1% wt. concentration in PEG200 are given in Table 1. Hydrodynamic sizes of CB-SiPEG additives (154-198 nm) dispersed in PEG200 are considerably smaller than those of pristine CB, both alone (678 nm) and with unbound SiPEG (902 nm). Polydispersity index (PDI) values for CB-SiPEG dispersions range between 0.04 and 0.12 whereas for pristine CB the values increase to 0.2-0.4. However, it is worth mentioning that DLS measurements of pristine CB dispersions do not meet required quality standards due to the presence of agglomerates and sedimentation and therefore can only be regarded as an evidence to support the poor dispersion of the non-functionalized additive. For CB-SiPEG dispersions, the hydrodynamic sizes are 3-4 times larger than the primary sizes of CB particles (~50 nm), which could be partly due to contribution from the long grafted SiPEG chains but mainly the result of interparticle interaction by hydrogen bonding between hydroxyl groups and oxyethylene units of grafted SiPEG chains in PEGylated CB. However, similar increase of hydrodynamic size versus primary particle size (2-3 fold) was also noted for non-functionalized CB dispersed in a mineral oil and was attributed to slight agglomeration of individual particles [14].On the other hand, hydrogen bonding interactions can also take place between hydroxyl groups and oxyethylene units of CB-SiPEG and PEG200 lube oil, enabling the excellent dispersion of PEGylated CB. The good additive dispersion and high degree of interaction between additive and oil will certainly contribute to the improved friction performance of CB-SiPEG/PEG200 blends. Chemical

coupling between CB-SiPEG and PEG200 lube oil facilitates intercalation of PEG200 chains between PEGylated CB additives, favoring lubrication as shear can take place between CB-SiPEG and PEG200. The remarkable influence of additive-oil interactions on the lubrication performance of PEG blends has also been shown for reduced graphene oxides with different functional groups by Gupta et al. [7]. In the case of soot, the dissimilar frictional characteristics encountered in different diesel engine oils have also been correlated with particle size distribution and presence of aggregates [40].

Once demonstrated the improved lubricating performance of CB-SiPEG/PEG200 blends, a series of PEGylated CB with five different SiPEG grafting ratios were investigated as friction and wear-reducing additives in PEG200 at a same concentration (1 % wt.). At this low additive concentration, the dynamic viscosity of the five CB-SiPEG/PEG200 blends at 25ºC was 53 ± 1 mPa s regardless of the additive composition, which is roughly the same as that of the PEG200 base oil (51 mPa s). Average friction coefficient values (from three replicates) for two 100Cr6 steel sliding surfaces lubricated with the different CB-SiPEG/PEG200 blends are given in Table 1. Detailed friction data (evolution of friction coefficient with time) for the five blends with different composition CB-SiPEG additives are shown in Figure S5. In general, the best lubricating performance corresponds to the additives with lower SiPEG grafting ratios, with steady-state friction coefficient values of 0.082 ± 0.005 (CB-SiPEG49), 0.075 ± 0.006 (CB-SiPEG61) and 0.085 ± 0.007 (CB-SiPEG71), which represent 29%, 35% and 26% reductions, respectively with respect to that of neat PEG200 base oil (0.115). On the contrary, PEGylated CB additives with high SiPEG content (> 75%) exhibit moderate friction coefficient reductions (3-4%). The lubrication performance trends for the five PEGylated CB additives with different CB:SiPEG ratios can be better visualized in Figure 5A, where average friction coefficient values are plotted vs. total CB content in the PEG200 oil. The values at 1% CB refer to blends with pristine (non-PEGylated) CB and are only included as a reference for comparison. As can be seen, there is an optimal additive composition (CB-SiPEG61) that

corresponds to only 0.39% wt. CB concentration in the lubricant blend. PEGylated CB additives with lower and higher CB content lead to lubricant blends with less pronounced friction performance improvement with respect to that of neat PEG200. It is worth mentioning that blends of CB-SiPEG additives with different CB:SiPEG ratios but a same total CB concentration exhibit different lubricating performance. Thus, the low friction coefficient (0.082) of the 1% CB-SiPEG49/PEG200 blend (with 0.51% wt. CB) could not be attained with a 2% CB-SiPEG76/PEG200 blend (with 0.48% wt. CB), whose performance was only slightly better than the same blend with 1% of the additive (CoF = 0.105), as shown in supporting information, Figure S6.

Hence, the results indicate that the lubricating properties of the blends are mainly governed by the chemical composition of the additive rather than CB concentration. Apparently, all PEGylated CB additives are well dispersed in PEG200 and the five CB-SiPEG(1% wt.)/PEG200 blends seem very homogenous (photographs in Figure 5B) with no traces of sediment nor visible agglomerates as in the case of pristine CB blends. However, DLS measurements reveal differences in particle size distribution for the different CB-SiPEG additives in PEG200 (supporting information, Figure S4). Overall, the hydrodynamic particle size in PEG200 oil (Table 1) tends to increase with SiPEG grafting ratio and the best lubrication performance corresponds to CB-SiPEG/PEG200 blends with the smallest hydrodynamic particle size. A similar improvement of lubrication capacity with decreasing hydrodynamic particle size was also noted for graphite particles dispersed in a mineral oil by Hwang et al. [14]. In the case of CB-SiPEG/PEG200 blends, taking into account all possible interactions between functional groups in additive and oil, CB-SiPEG61 (with 61% SiPEG grafting ratio) seems to be the optimal composition to balance the amount of additive-oil interactions for a good dispersion and additive-additive interactions for minimal hydrodynamic particle size.

3.3. Wear properties of PEG blends with PEGylated CB additives

The wear tracks in the disks after pin-on-disk tribology tests with the different lubricant blends were examined by optical and confocal microscopy (Figure 6). Although all blends had 1% wt. additive concentration, the width and depth of the tracks varied considerably with the blend composition. For a better comparison of the antiwear properties of each blend, specific wear rate (k) average values are given in Table 1 and plotted in Figure 5A as a function of total CB concentration in the lubricant blend. Overall, similar trends for wear rates and friction coefficients were noted. Thus, PEG200 blends containing 1% wt. SiPEG (Figure 6b), 1% wt. pristine CB (Figure 6c) or a 0.5% wt. pristine CB and 0.5% wt. unbound SiPEG mixture (Figure 6d) exhibited roughly the same antiwear performance as neat PEG200 (Figure 6a), all displaying k values of $1.0\text{-}1.1\cdot10^{-6}$ $mm^3\ N^{-1}\ m^{-1}$. That is, pristine CB, alone or with unbound SiPEG, did not behave as a friction-reducing nor antiwear additive in PEG200 under the tribo-conditions used, in agreement with reports where CB was investigated in different formulated engine lubricants to simulate the effect of soot contamination [18,19]. On the contrary, blends of the different PEGylated CB additives showed a composition-dependent antiwear performance comparable to their lubrication capacity. In the case of CB-SiPEG additives with the lowest SiPEG grafting ratios (49-71%), wear track width and depth was considerably reduced (Figure 6e-g) compared to that of neat PEG200 (Figure 6a). Thus, specific wear rates using PEG200 blends with 1% wt. of these additives were $4.4\cdot10^{-7}$ $mm^3\ N^{-1}\ m^{-1}$ (CB-SiPEG49), $3.7\cdot10^{-7}$ $mm^3\ N^{-1}\ m^{-1}$ (CB-SiPEG61) and $5.5\cdot10^{-7}$ $mm^3\ N^{-1}\ m^{-1}$ (CB-SiPEG71), values that represent remarkable reductions (61%, 67% and 52%, respectively) with respect to neat PEG200 oil.

Interestingly, blends of CB-SiPEG additives with higher SiPEG content (≥ 76%) showed clearly better antiwear performance than PEG200 oil, with significant wear rate reductions (25-27%) despite their moderate friction coefficient improvement (3-4%). It is noteworthy to

underline the remarkable wear-protection capacity of CB-SiPEG given the well-established wear-promoting role of soot in engine oils [41]. Moreover, it has been reported that wear with base oils containing CB further increases in the presence of dispersants [18]. The improved lubricating and wear protection properties of CB-SiPEG/PEG200 blends compared to neat PEG200 or CB/PEG200 blends could result from different factors: (1) better additive dispersion and hydrogen bonding interactions between additive and oil that facilitate SiPEG/PEG200 chain intercalation and hence more effective shear mobility between additive and oil intercalated chains; (2) improved adhesion properties on steel surfaces leading to formation of a higher-strength protective tribofilm as a result of hydrogen bonding interactions between SiPEG grafted oxyethylene units in the additive and hydroxides present at the steel surface.

In this regard, chemical analysis of the wear track was carried out by EDS to provide evidence of tribofilm formation during the tribo-tests with CB-SiPEG/PEG200 lubricating blends. The disks were thoroughly washed by ultrasonication in different solvents to remove residual traces of lubricant or wear debris. Despite the washing, spherical black spots (marked with arrows) were clearly seen inside the wear track grooves for the best-performing lubricating blends (Figure 6). EDS analysis of several regions inside the wear track (Figure 7A) from tribo-tests with the optimal lubricating blend (1% wt. CB-SiPEG61/PEG200) reveals an increase in carbon and oxygen content (12.4 ± 1.8% at. C and 5.0 ± 0.5% at. O) inside the wear track with respect to the content of a virgin (non-exposed to the lubricant) 100Cr6 steel disk surface (11.3 ± 1.7% at. C and 2.1 ± 0.3% at. O) or the content inside the wear track of surfaces lubricated with PEG200 base oil alone (11.4 ± 1.4% at. C and 3.3 ± 0.4% at. O). Although EDS is not a surface-sensitive technique and subsurface contribution is important, the higher carbon and oxygen contents inside the wear track were not detected in neighboring regions outside the track exposed to the lubricating blends, with a composition (10.7 ± 1.6%

at. C and 2.5 ± 0.2% at. O) similar to that of the virgin 100Cr6 steel surface. This would support the deposition of chemisorbed CB-SiPEG61 nanoparticles (with XPS chemical composition in at.% of 77.6% C, 19.8% O and 2.6% Si) on the surface of the wear track forming a protective tribofilm that lowers friction and wear between the tribo-pairs. Silicon was also detected on surfaces lubricated with CB-SiPEG61/PEG200 (inside and outside the wear track) but the content was roughly the same as that present in the virgin 100Cr6 steel surface (0.40 ± 0.15% at) and therefore cannot be attributed to deposited CB-SiPEG61 whose Si content is too low to be resolved from subsurface contribution. On the other hand, the higher relative oxygen-to-carbon content inside the wear track (O/C = 0.40) compared to the pristine CB-SiPEG61 additive (O/C = 0.26) and the virgin 100Cr6 steel surface (O/C = 0.19) points to oxidation of the additive during the tribology test, as has also been reported for graphene or nanodiamond additives in PEG or ethylene glycol lubricants [7, 42]. Additionally, Raman spectroscopy corroborated CB-SiPEG61 deposition inside the grooves, as particles in the track featured the characteristic Raman spectra of CB (Figure 7B) with the graphitic G band at a shift of ~1575 cm^{-1} and the disorder D band from the carbon atoms close to the edge of the graphite sheets at ~1360 cm^{-1}. On the contrary, the Raman fingerprint of CB could not be detected in regions outside the track (Figure 7B), nor was identified on surfaces (inside or outside wear tracks) where PEG200 alone was used as lubricant (Figure 7C). In this case, only a very weak intensity signal was measured inside the wear track at Raman shifts characteristic of PEG200 (510 and 1250 cm^{-1}).

3.4. Stability of optimal PEG/CB-SiPEG blends

As it is well known that additive concentration plays an important role in lubricant performance, the friction behavior of PEG200 blends with different concentrations of the best lubricating additive (CB-SiPEG61) was investigated with the aim of identifying the optimal blend composition for stability testing. The evolution of friction coefficients with time for

100Cr6 steel sliding surfaces lubricated with neat PEG200 and the different PEG200/CB-SiPEG61 blends is compared in Figure S7A. Figure S7B shows average (n=2) steady-state values with the standard deviation for each concentration. PEG200/CB-SiPEG61 blends exhibit typical concentration-dependent lubricating performance reported for PEG or ethylene glycol blended with other carbon nanoadditives such as nanodiamonds or graphite [42, 43]. That is, at the beginning of the tribo-test (i.e. t < 50 s), similar friction coefficient values were measured for all blends (~0.09). However, as the test continues, friction coefficient values gradually increase for blends with low CB-SiPEG concentrations (< 1% wt.) until reaching a steady-state value equal to that of neat PEG200 oil (0.12). This poor lubricating performance time stability of less-concentrated blends (< 1% wt.) indicates that the amount of friction-reducing additive is too small to fill properly the contact interface during the whole sliding test. On the contrary, the lubrication efficiency of blends with too high CB-SiPEG61 concentrations (2% wt.) was reduced, most likely due to particle-particle collisions that produce defects and wear at the contact interface. At the optimal additive concentration (1% wt.) the low friction coefficient (0.075) was maintained during the entire test due to formation of a stable protective tribo-film as discussed above.

Finally, the lubricating performance stability of the optimal blend was assessed by pin-on-disk tribology tests under the same conditions using the same blend 10 weeks after preparation. Visual inspection did not reveal differences in the CB-SiPEG61/PEG200 blend after 10 weeks (photographs in Figure 8), as no sedimentation occurred after this time. Indeed, the low friction coefficient remained stable (R.S.D. = 5%) in tests conducted with the same blend 10 weeks and 6 months after preparation, corroborating the stable lubricating performance of aged blends. EDS analysis of the wear tracks of tribo-tests with aged CB-SiPEG61/PEG200 blends also reveals high carbon and oxygen content (13.0 ± 2.4% at. C and 7.6 ± 1.6% at. O) inside the tracks, indicating the deposition of chemisorbed CB-SiPEG additives and formation of an effective tribo-film.

DLS measurements of fresh and aged blends (Figure 8) did not show significant differences in hydrodynamic particle size distributions of CB-SiPEG61 additive at 1% wt. in PEG200, which decreased from 155 ± 5 nm (PDI = 0.100) to 140 ± 3 nm (PDI=0.075) after 10 weeks, remaining stable later on for at least 6 months. Likewise, very small particle size reductions (around 20-30 nm) with time were measured for the other CB-SiPEG/PEG200 blends with different SiPEG grafting ratios. These findings highlight the efficiency of PEGylation as a route to achieve stable CB dispersion in a polar base oil, with small particle size and polydispersity preserved over long periods of time. The results illustrating the performance stability of lubricating blends on month-timescale are inspiring, as often reports on lubricant formulations with solid additives lack stability studies or show only few hours/days results.

4. Conclusions

(1) PEG chains were covalently grafted on hydroxylated CB by silanization with a PEG-terminated trimethoxysilane and synthesis conditions were varied to yield a series of PEGylated CB additives with different SiPEG grafting ratios. (2) Grafted PEG chains enhance CB dispersibility in PEG200 lube oil due to formation of hydrogen bonds between hydroxyl groups and oxyethylene units of CB-SiPEG and PEG200. (3) Hydrodynamic particle sizes of CB-SiPEG dispersed in PEG200 were considerably smaller than those of pristine CB alone and with free SiPEG added. (4) Chemical interactions between CB-SiPEG and PEG200 lube oil facilitates intercalation of PEG200 chains between PEGylated CB additives, favoring lubrication in ball-on-disk tribometer tests with 100Cr6 steel sliding surfaces. (5) At the optimal SiPEG content (61% wt.), friction coefficient and specific wear rate were reduced with CB-SiPEG/PEG200 by 35% and 67% respectively, compared to PEG200 alone whereas pristine CB/PEG200 blends at the same concentration did not show friction-reducing or antiwear capacity. (6) Increase in carbon and oxygen content inside the wear track together

with the Raman fingerprint of the additives supports the deposition of chemisorbed CB-SiPEG nanoparticles on the wear track surface forming a protective tribofilm that lowers friction and wear between the tribo-pairs. (7) Particle size distribution and lubricating performance of the blends is preserved 6 months after preparation, highlighting a remarkable additive dispersion stability.

Acknowledgements

Financial support from Diputación Foral de Gipuzkoa (OIL project, ref. 188/2017) is gratefully acknowledged.

References

[1] Rizvi SQA. A comprehensive review of lubricant chemistry, technology, selection and design, Baltimore: ASTM International; 2009.

[2] Kobayashi M, Koide T, Hyon S-H. Tribological characteristics of polyethylene glycol (PEG) as a lubricant for wear resistance of ultra-high-molecular-weight polyethylene (UHMWPE) in artificial knee joint. J Mech Behav Biomed Mater 2014;38:33-8.

[3] Minami I. Molecular science of lubricant additives. Appl Sci 2017;7:445.

[4] Yao MH, Liang YM, Xia YQ, F. Zhou F. Bisimidazolium ionic liquids as the high-performance antiwear additives in poly(ethylene glycol) for steel−steel contacts. ACS Appl Mater Interfaces 2009;1(2):467–71.

[5] Wang B, Tang W, Lu H, Huang Z. Ionic liquid capped carbon dots as a high-performance friction-reducing and antiwear additive for poly(ethylene glycol). J Mater Chem A 2016;4: 7257-65.

[6] Shen M, Luo J, Wen S. The tribological properties of oils added with diamond nano-particles. Tribol Trans 2001;44:494-8.

[7] Gupta B, Kumar N, Panda K, Kanan V, Joshi S, Visoly-Fisher I. Role of oxygen functional groups in reduced graphene oxide for lubrication. Sci Rep 2017;7:45030.

[8] Shang W, Cai T, Zhang Y, Liu D, Liu S. Facile one pot pyrolysis synthesis of carbon quantum dots and graphene oxide nanomaterials: All carbon hybrids as eco-environmental lubricants for low friction and remarkable wear-resistance. Tribol Int 2018;118:373-80.

[9] Savage RH. Graphite lubrication. J Appl Phys 1948;19(1):1–10.

[10] Zhang ZJ, Simionesie D, Schaschke C. Graphite and hybrid nanomaterials as lubricant additives. Lubricants 2014;2:44-65.

[11] Joly-Pottuz L, Ohmae N. Carbon-based nanolubricants. In: Martin JM, Ohmae N, editors. Nanolubricants, Chapter 3, Chichester UK; John Wiley & Sons; 2008, 93–147.

[12] Zhai W, Srikanth N, Kong LB, Zhou K. Carbon nanomaterials in tribology. Carbon 2017;119:150-71.

[13] Baik S, Yoon D, Lee HI, Kim JM, Lee GS, Lee YZ. Frictional performances of activated carbon and carbon blacks as lubricant additives. Tribol Trans 2008;52:133-37.

[14] Hwang Y, Lee C, Choi Y, Cheong S, Kim D, Lee K, Lee J, Kim SH. Effect of the size and morphology of particles dispersed in nano-oil on friction performance between rotating discs. J Mech Sci Technol 2011;25:2853-7.

[15] O'Halloran R. Carbon black lubricating grease. US patent 2696469A, 1954.

[16] Lalla ES. Gear lubricant comprising carbon black. US patent 8853138B1, 2014.

[17] Mabuchi Y, Nakagawa A. Nanoparticle-containing lubricating oil compositions, US patent 9023771B2, 2015.

[18] Salehi FM, Khaemba DN, Morina A, Neville, A. Corrosive–abrasive wear induced by soot in boundary lubrication regime. Tribol Lett 2016;63:1-11.

[19] Hu E, Hu X, Liu T, Fang L, Dearn KD, Xu H. The role of soot particles in the tribological behavior of engine lubricating oils. Wear 2013;304:152-61.

[20] Jenei IZ, Dassenoy F, Epicier T, Khajeh A, Martini A, Uy D, Ghaednia H, Gangopadhyay A. Mechanical response of gasoline soot nanoparticles under compression: An in situ TEM study. Tribol Int 2019;131:446-53.

[21] Motamen Salehi F, Morina A, Neville A. Zinc dialkyldithiophosphate additive adsorption on carbon black particles. Tribol Lett 2018;66:1-7

[22] Van Os NM. Nonionic surfactants: organic chemistry, Volume 72, New York; Marcel Dekker Inc.; 1998.

[23] Kronberg B, Holmberg K, Lindman B. Surface chemistry of surfactants and polymers. UK; Wiley; 2014.

[24] Kim H, Park K, Lee MY. Biocompatible dispersion methods for carbon black. Toxicol Res 2012;28:209-16.

[25] Han Y, Hwang G, Park S, Gomez-Flores A, Jo E, Eom I-C, Tong M, Kim H-J, Kim H. Stability of carboxyl-functionalized carbon black nanoparticles: the role of solution chemistry and humic acid. Environ Sci: Nano 2017;4:800-10.

[26] Leistenschneider D, Zürbes K, Schneidermann C, Grätz S, Oswald S, Wegner K, Klemmed B, Giebeler L, Eychmüller A, Borchardt L. Mechanochemical functionalization of carbon black at room temperature. C 2018;4:14.

[27] Wang H, Xu H, Jia W, Ren S. Functionalized carbon black nanoparticles used for separation of emulsified oil from oily wastewater. J. Disper Sci Technol 2018;39:497-506.

[28] Lee S, Eum CH, Kim WJ. Surface modification of carbon black using polymer resin synthesized by a phenyl radical reaction. J Korean Chem Soc 2016;60:289-91.

[29] Zhou G, Xu X, Wang S, He X, He W, Su X, Wong CP. Surface grafting of epoxy polymer on CB to improve its dispersion to be the filler of resistive ink for PCB. Results Phys 2017;7:1870-7.

[30] Flenniken CL, Menashi J, Whitehouse RS. Polyethylene glycol treated carbon black and compounds thereof. US patent 5725650A, 1998.

[31] Pritchard JE, Robbins AL. Dispersion of carbon black in polyolefins. US patent 3206419A,1960.

[32] Kim WS, Paik HJ, Bae JW, Kim W. Effect of polyethylene glycol on the properties of styrene-butadiene rubber/organoclay nanocomposites filled with silica and carbon black. J Appl Polym Sci 2011;122:1766-77.

[33] Lin JH, Chen HW, Wang KT, Liaw FH. A novel method for grafting polymers on carbon black. J Mater Chem 1998;8:2169-73.

[34] Pradhan BK, Sandle NK. Effect of different oxidizing agent treatments on the surface properties of activated carbons. Carbon 1999;37:1323-32.

[35] Ahmed GS, Gilbert M, Mainprize S, Rogerson M. FTIR analysis of silane grafted high density polyethylene. Plast Rubber Compos 2009;38:13-20.

[36] Diez-Pascual AM, Diez-Vicente AL. PEGylated boron nitride nanotube-reinforced poly(propylene fumarate) nanocomposite biomaterials. RSC Adv 2016;6:79507-19.

[37] Kinoshita K. Carbon: electrochemical and physicochemical properties. New York; Wiley; 1988, 86–116.

[38] Li ZQ, Lu CJ, Xia ZP, Zhou Y, Luo, Z. X-ray diffraction patterns of graphite and turbostratic carbon. Carbon 2007;45:1686-95.

[39] Layek RK, Nandi AK. A review on synthesis and properties of polymer functionalized graphene. Polymer 2013;54:5087-103.

[40] Liu C, Nemoto S, Ogano S. Effect of soot properties in diesel engine oils on frictional characteristics. Tribol Trans 2003;46:12-8.

[41] Green DA, Lewis, R. The effects of soot-contaminated engine oil on wear and friction: a review. Department of Mechanical Engineering, University of Sheffield; 2008.

[42] Elomaa O, Hakala TJ, Myllymäki V, Oksanen J, Ronkainen H, Singh VK et al. Diamond nanoparticles in ethylene glycol lubrication on steel-steel high load contact. Diamond Relat Mater 2013;34:89-94.

[43] Gupta B, Panda K, Kumar N, Melvin AA, Dash S, Tyagi AK. Chemically grafted graphite nanosheets dispersed in poly(ethylene-glycol) by γ–radiolysis for enhanced lubrication. RSC Adv 2015;5:53766-75.

Captions

Figure 1. Scheme of the CB PEGylation reaction.

Figure 2. (A) FTIR transmission spectra, (B) TGA curves, (C) XRD spectra and (D) XPS general survey spectra (with chemical composition in at. %) of pristine CB (a), CB-ox (b), SiPEG (c) and CB-SiPEG additives with different SiPEG grafting ratios: 49% (d), 61% (e), 71% (f), 76% (g) and 80% (h).

Figure 3. FESEM micrographs and photographs of (a) pristine CB, (b) CB-SiPEG49 and (c) CB-SiPEG80 samples.

Figure 4. Friction coefficients of 100Cr6 steel disks lubricated with neat PEG200, 1% CB in PEG200, 1% SiPEG in PEG200, 1% CB-SiPEG49 in PEG200 and a blend of CB (0.5%) and SiPEG (0.5%) in PEG200. Inset shows photographs of the PEG200 formulations with 1% of each additive: CB, CB-SiPEG49 and the blend of CB and unbound SiPEG.

Figure 5. (A) Average friction coefficients and specific wear rates of 100Cr6 steel disks lubricated with PEG200 blends containing 1% wt. CB-SiPEG additives with different SiPEG grafting ratios, plotted as a function of total CB concentration in the blend. (B) Photographs of 1% wt. CB-SiPEG/PEG200 blends with the different SiPEG grafting ratios indicated in the figure.

Figure 6. Optical images and profiles of wear tracks on 100Cr6 steel disks lubricated with neat PEG200 and PEG200 blends with 1% wt. of the different additives indicated in the figure.

Figure 7. Optical image with EDS analysis (A) and Raman maps with corresponding spectra in regions inside and near the wear track on 100Cr6 steel disks after pin-on-disk tribology tests with 1% wt. CB-SiPEG61/PEG200 lubricating blend (B) and PEG200 base oil alone (C).

Raman maps were generated by plotting the integrated signal intensity of the D band of CB (B) and the band around 1250 cm^{-1} for PEG200 (C).

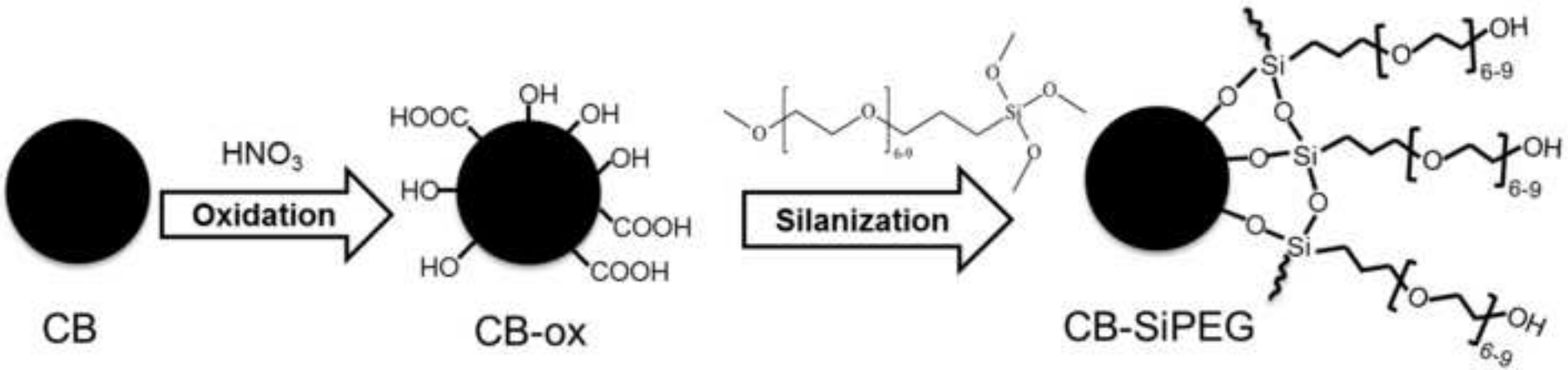
Figure 8. Size distribution of CB-SiPEG6 additives in fresh and aged (> 10-week old) PEG200 blend measured by DLS and photographs of the blends.

Table 1. Chemical and tribological properties of CB-SiPEG additives, PEG200 and PEG200 dispersions at 1% wt. additive content

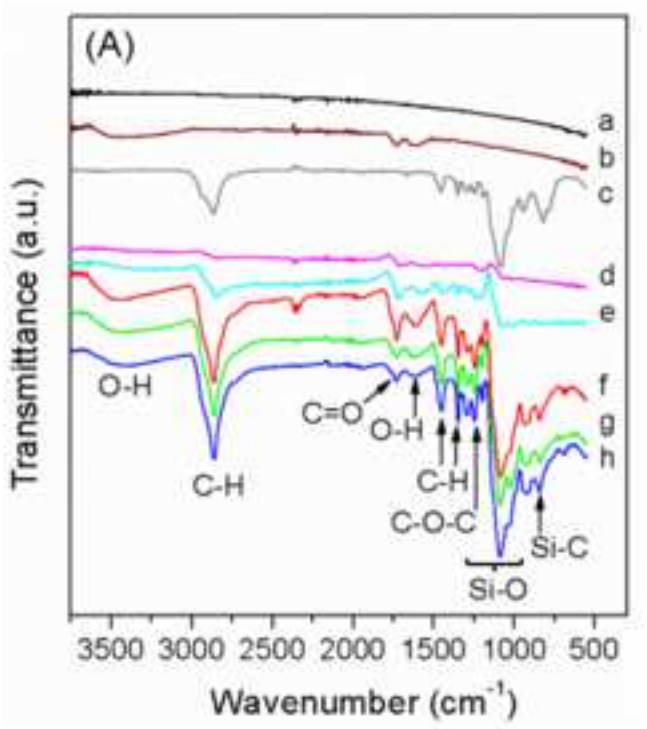
Sample	% SiPEG	% CB	XRD (002) peak (2θ)	Friction coefficient	Wear rate ($mm^3 N^{-1}m^{-1}$)	Hydrodynamic particle size (nm)
CB-SiPEG49	49	51	23.5º	0.082	$4.4 \cdot 10^{-7}$	158
CB-SiPEG61	61	39	22.4º	0.075	$3.7 \cdot 10^{-7}$	154
CB-SiPEG71	71	29	21.9º	0.085	$5.5 \cdot 10^{-7}$	162
CB-SiPEG76	76	24	21.6º	0.110	$8.2 \cdot 10^{-7}$	194
CB-SiPEG80	80	20	21.1º	0.112	$8.5 \cdot 10^{-7}$	198
PEG200	-	-	-	0.115	$1.1 \cdot 10^{-6}$	-
CB	-	-	24.5º	0.110	$1.1 \cdot 10^{-6}$	680*
CB-ox	-	-	24.9º	-	-	-
CB + SiPEG	-	-	24.2º	0.115	$1.0 \cdot 10^{-6}$	902*

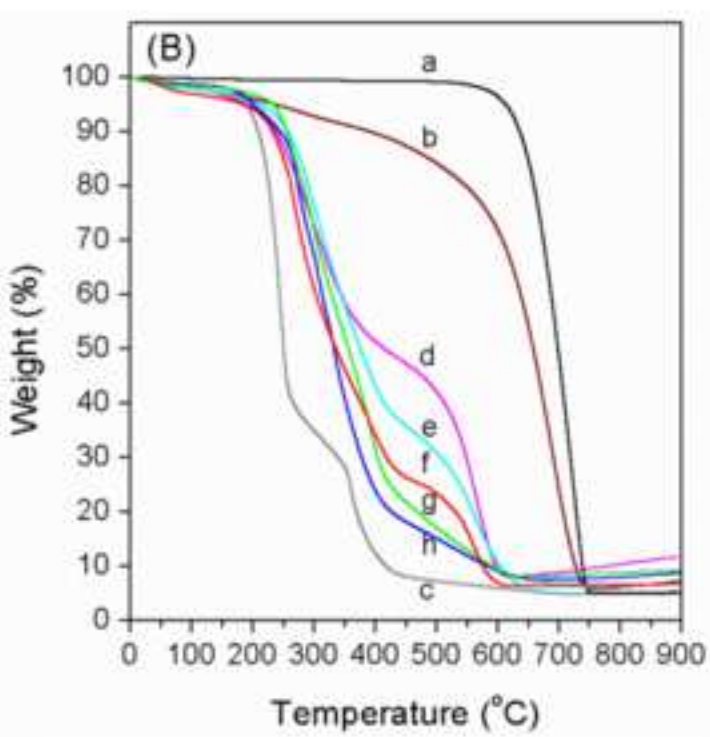
***** Poor quality DLS measurements (agglomerates and sedimentation)

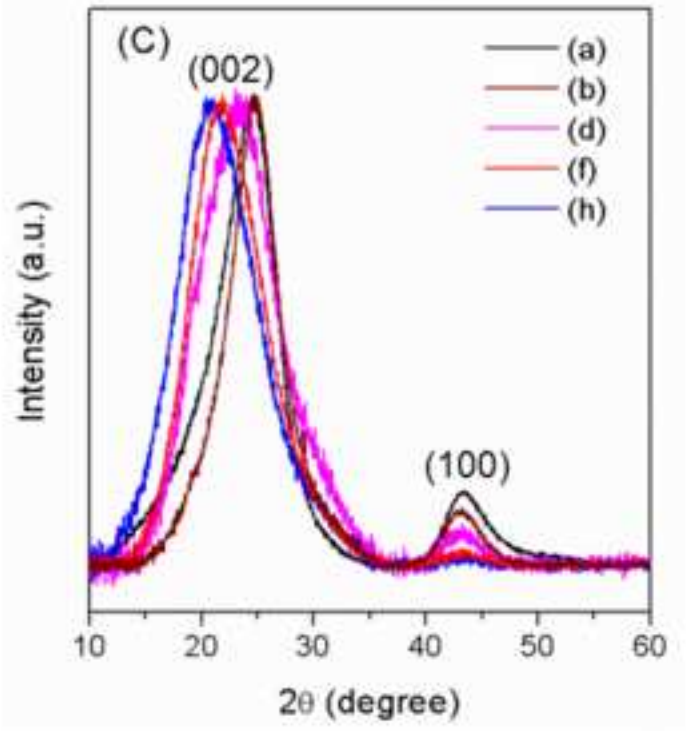
Figure(s)

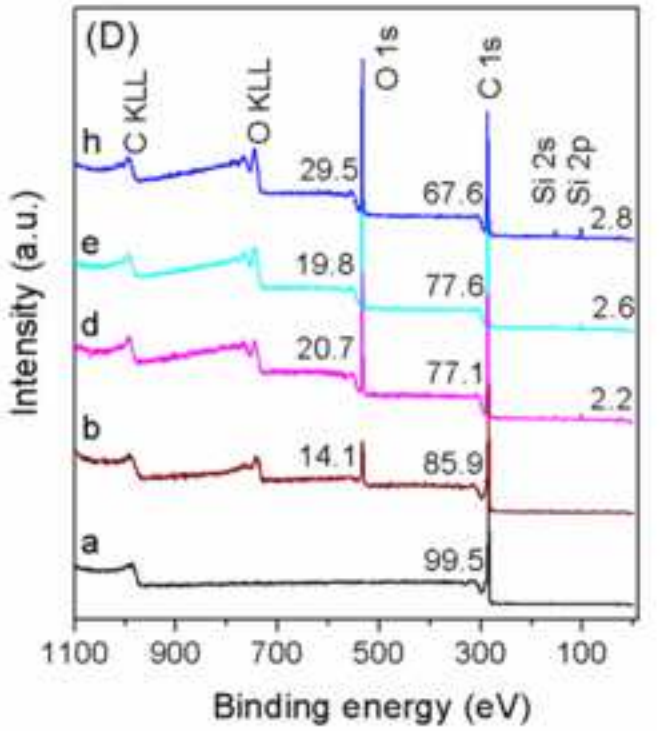

HNO3
Oxidation
HOOC
OH
OH
OH
HO
COOH
HO
COOH
Silanization
Si
OH
6-9
CB
CB-ox
CB-SiPEG

Figure(s)

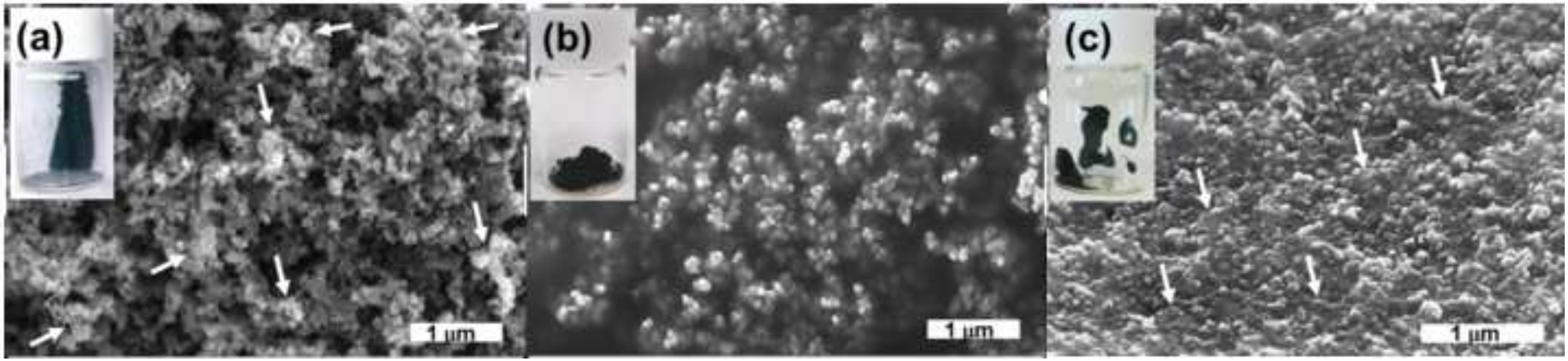

(A)
Transmittance (a.u.)
Wavenumber (cm^{-1})
3500 3000 2500 2000 1500 1000 500
a
b
c
d
e
f
g
h
O-H
C-H
C=O
O-H
C-H
C-O-C
Si-C
Si-O


(B)
Weight (%)
Temperature (°C)
0 100 200 300 400 500 600 700 800 900
100 90 80 70 60 50 40 30 20 10 0
a
b
c
d
e
f
g
h

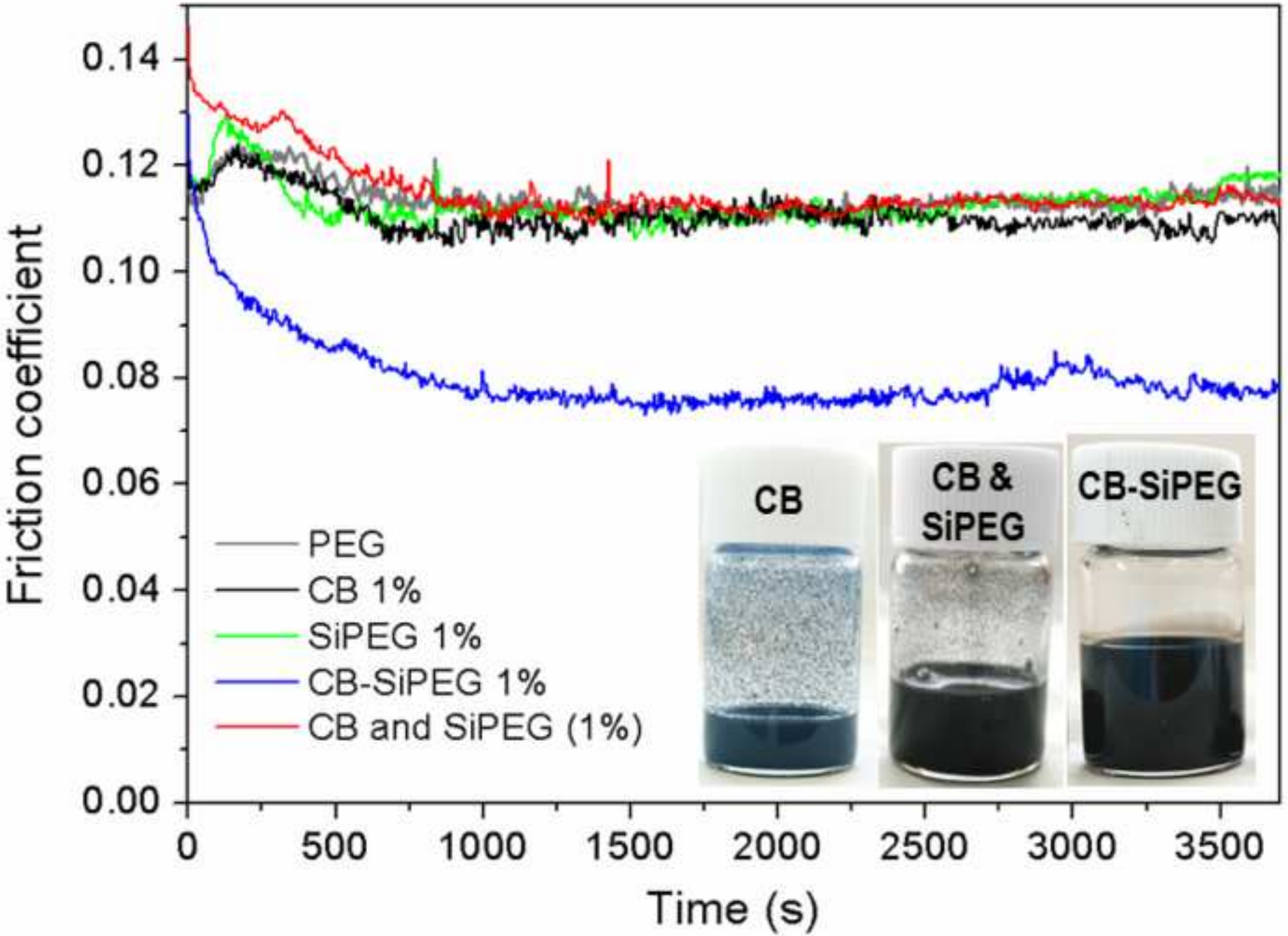

(C)
(002)
(100)
(a)
(b)
(d)
(f)
(h)
Intensity (a.u.)
2θ (degree)
10 20 30 40 50 60


(D)
C KLL
O KLL
O 1s
C 1s
Si 2s
Si 2p
h
e
d
b
a
29.5
67.6
2.8
19.8
77.6
2.6
20.7
77.1
2.2
14.1
85.9
99.5
Intensity (a.u.)
Binding energy (eV)
1100 900 700 500 300 100

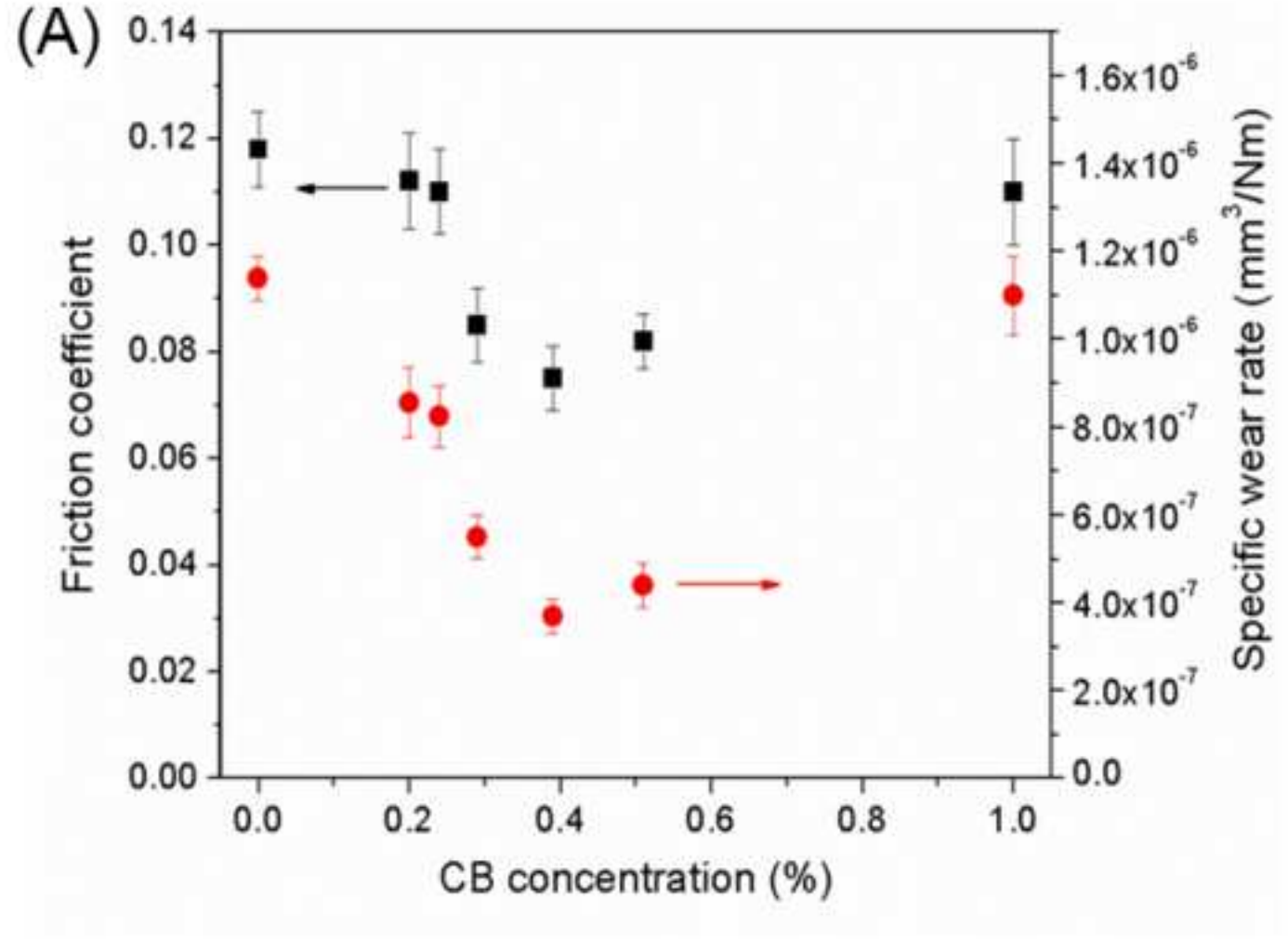
Figure(s)

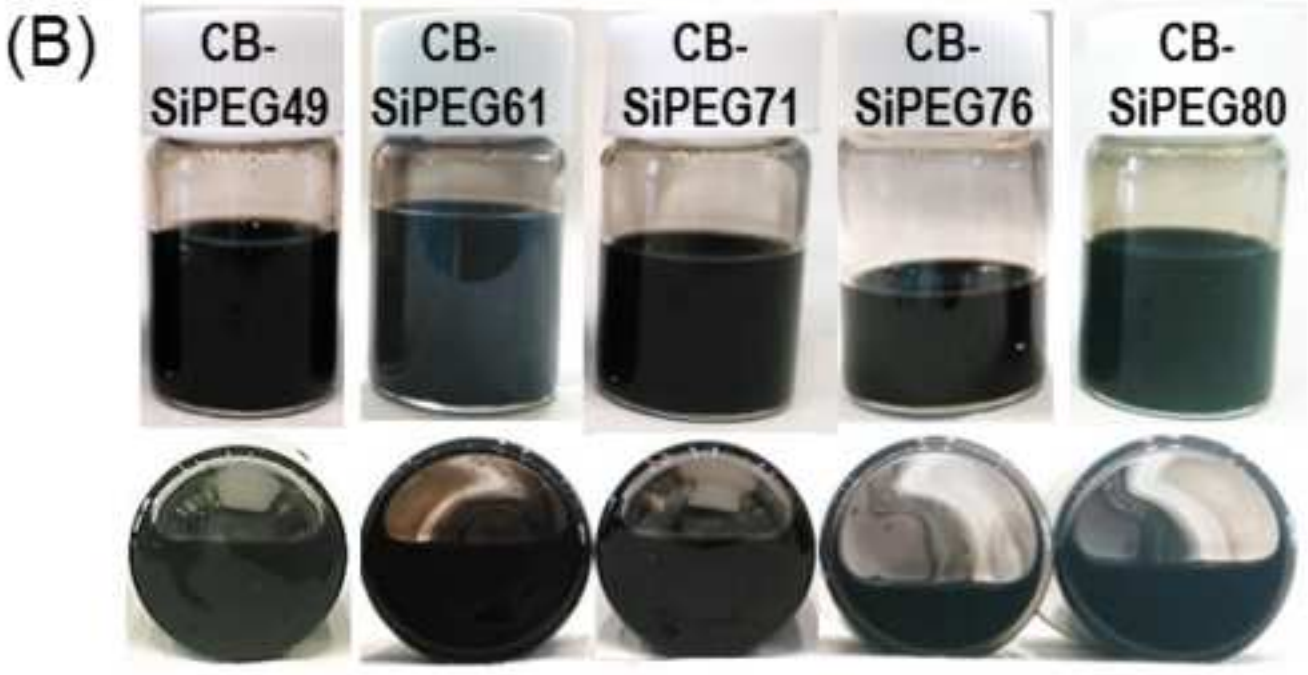


Figure(s)

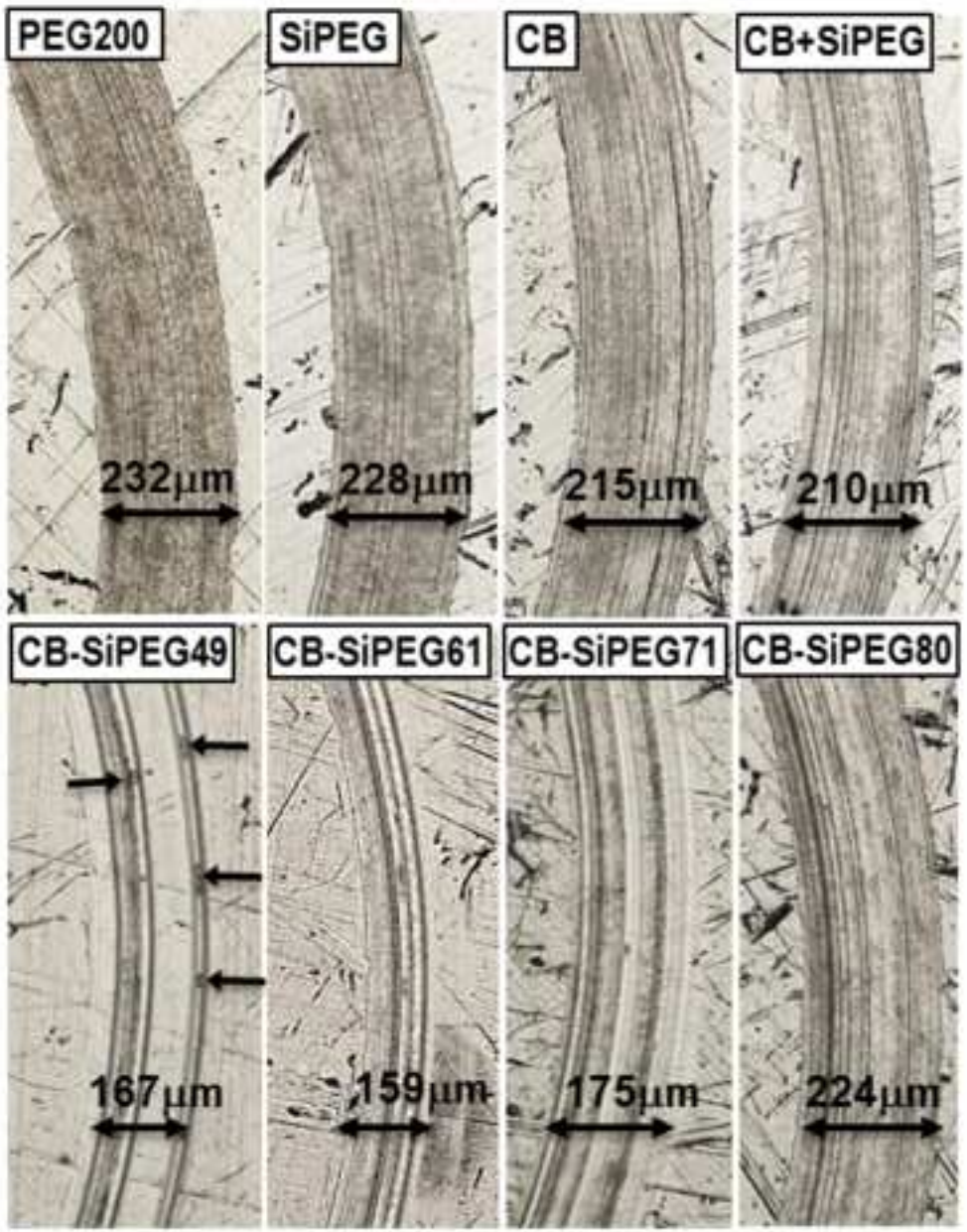

Friction coefficient
0.14
0.12
0.10
0.08
0.06
0.04
0.02
0.00
0
500
1000
1500
2000
2500
3000
3500
Time (s)
PEG
CB 1%
SiPEG 1%
CB-SiPEG 1%
CB and SiPEG (1%)
CB
CB &
SiPEG
CB-SiPEG

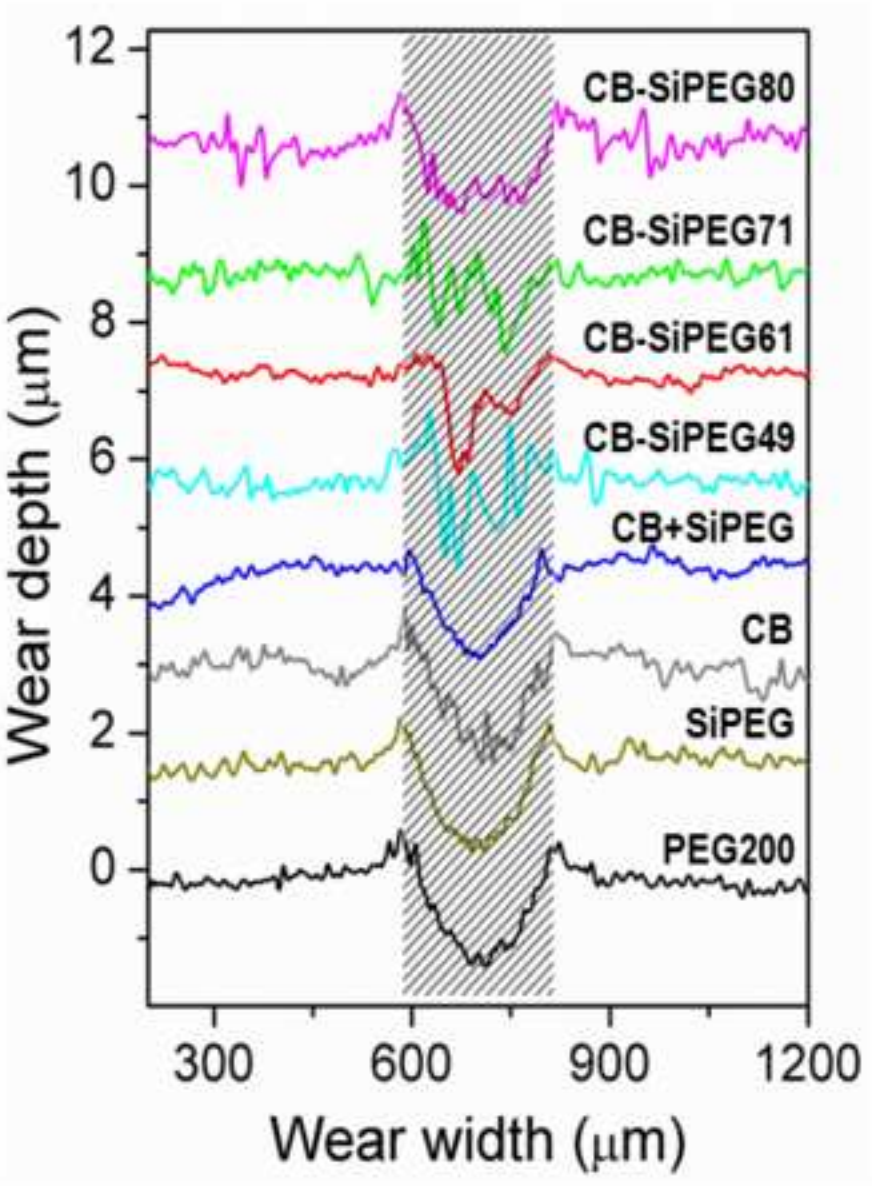
Figure(s)


(A)
Friction coefficient
Specific wear rate (mm³/Nm)
CB concentration (%)
0.14
0.12
0.10
0.08
0.06
0.04
0.02
0.00
1.6x10⁻⁶
1.4x10⁻⁶
1.2x10⁻⁶
1.0x10⁻⁶
8.0x10⁻⁷
6.0x10⁻⁷
4.0x10⁻⁷
2.0x10⁻⁷
0.0
0.0
0.2
0.4
0.6
0.8
1.0

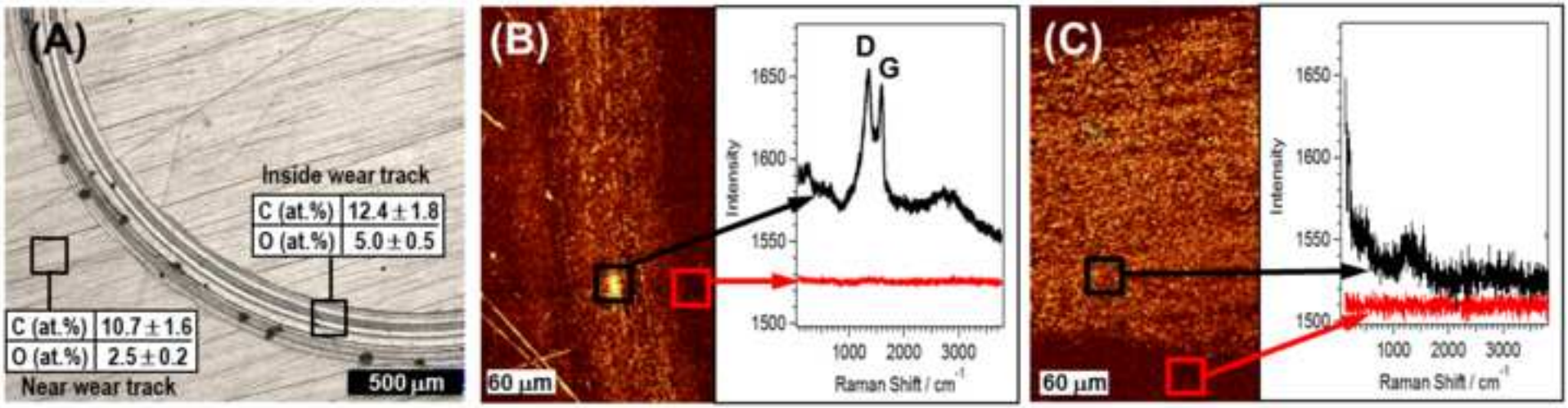

(B)
CB-SiPEG49
CB-SiPEG61
CB-SiPEG71
CB-SiPEG76
CB-SiPEG80

Figure(s)

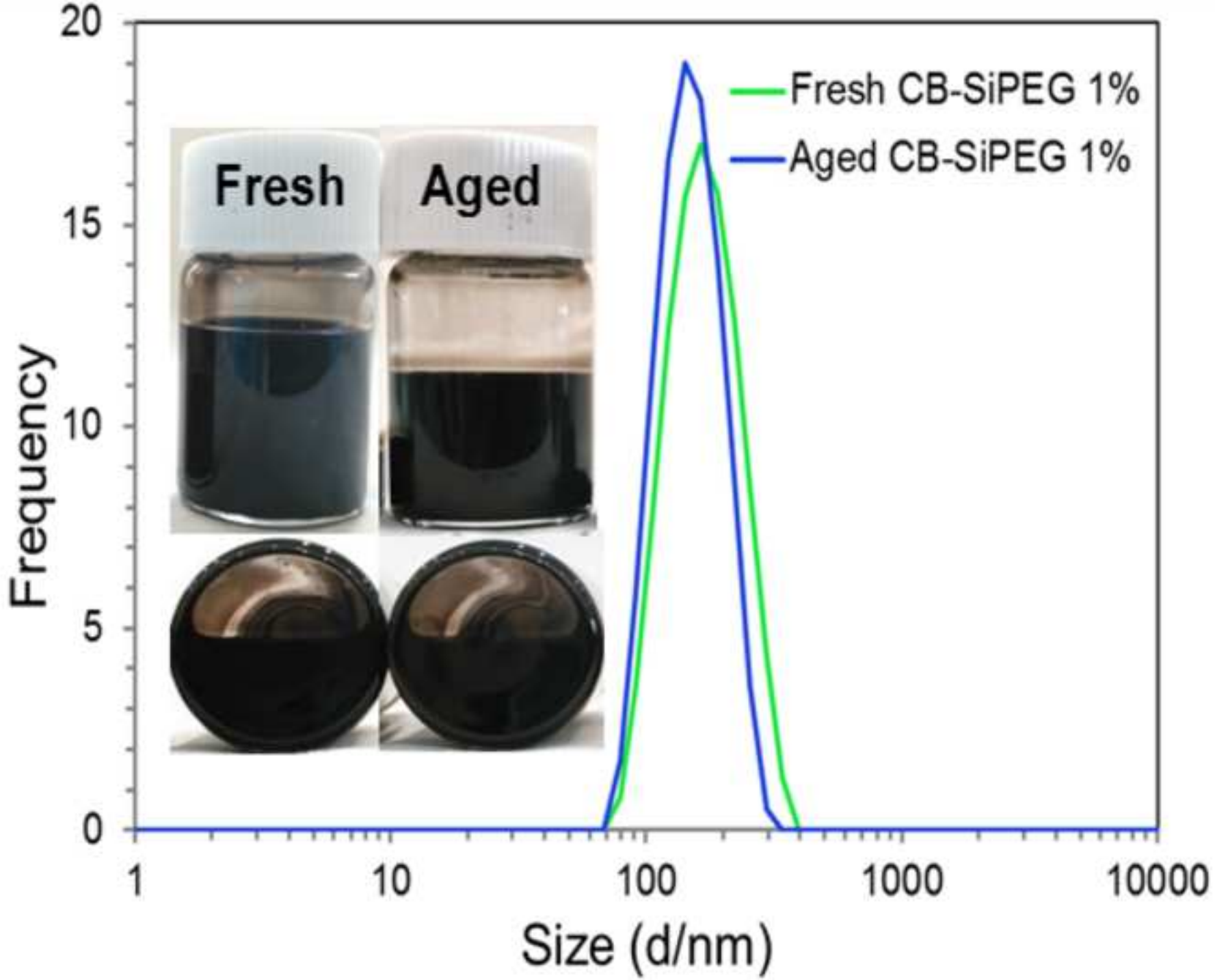

PEG200
SiPEG
CB
CB+SiPEG
232μm
228μm
215μm
210μm
CB-SiPEG49
CB-SiPEG61
CB-SiPEG71
CB-SiPEG80
167μm
159μm
175μm
224μm


Wear depth (μm)
Wear width (μm)
0
2
4
6
8
10
12
300
600
900
1200
CB-SiPEG80
CB-SiPEG71
CB-SiPEG61
CB-SiPEG49
CB+SiPEG
CB
SiPEG
PEG200

Figure(s)


(A)
Inside wear track
C (at.%) 12.4 ± 1.8
O (at.%) 5.0 ± 0.5
C (at.%) 10.7 ± 1.6
O (at.%) 2.5 ± 0.2
Near wear track
500 µm
(B)
60 µm
D
G
Intensity
1650
1600
1550
1500
1000 2000 3000
Raman Shift / cm-1
(C)
60 µm
Intensity
1650
1600
1550
1500
1000 2000 3000
Raman Shift / cm-1

Figure(s)


Fresh
Aged
Fresh CB-SiPEG 1%
Aged CB-SiPEG 1%
Frequency
Size (d/nm)
0
5
10
15
20
1
10
100
1000
10000

Companion Files
Click here to download Companion Files: Supporting information.docx

Supporting Information

PEGylated carbon black as lubricant nanoadditive with enhanced dispersion stability and tribological performance

Virginia Ruiz[a,*], Luis Yate[b], Judith Langer[b], Ivet Kosta[a], Hans J. Grande[a], Ramón Tena-Zaera[a]

[a]CIDETEC, Paseo Miramón 191, E-20014 Donostia-San Sebastián, Spain.

[b]CIC biomaGUNE, Paseo Miramón 192, E-20014 Donostia-San Sebastián, Spain.

[*]Corresponding author. Tel: +34-943-309022; E-mail: vruiz@cidetec.es

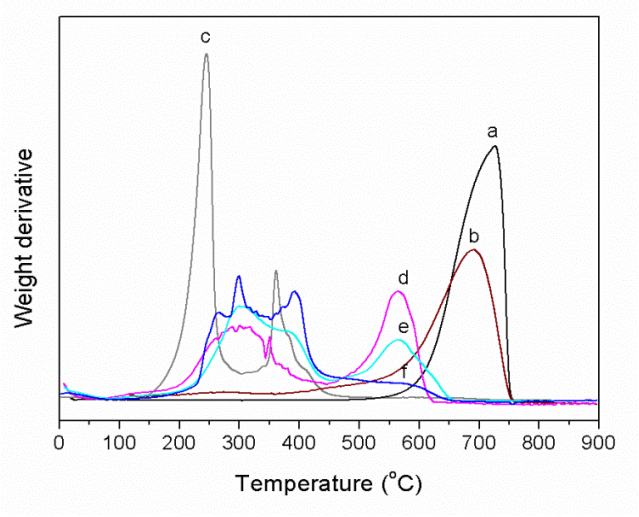


Figure S1. Derivative TGA under air atmosphere of pristine CB (a), CB-ox (b), SiPEG (c) and CB-SiPEG with 49% (d), 61% (e) and 80% (f) SiPEG grafting ratios.

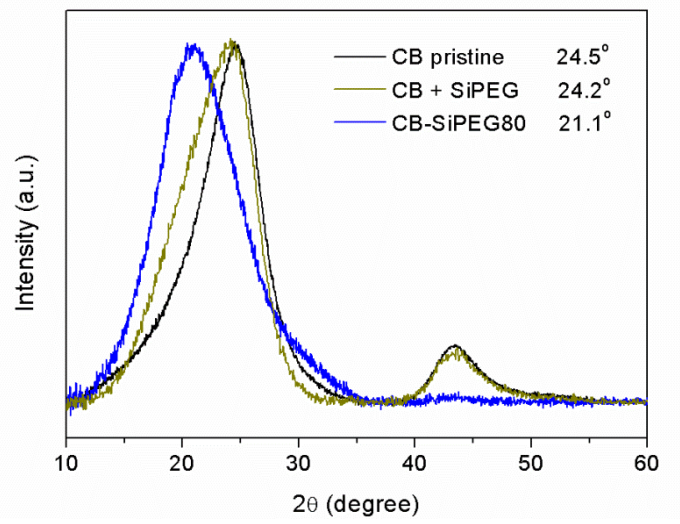


Figure S2. XRD of pristine CB, CB-SiPEG80 and a mixture (1:100) of CB and free SiPEG.

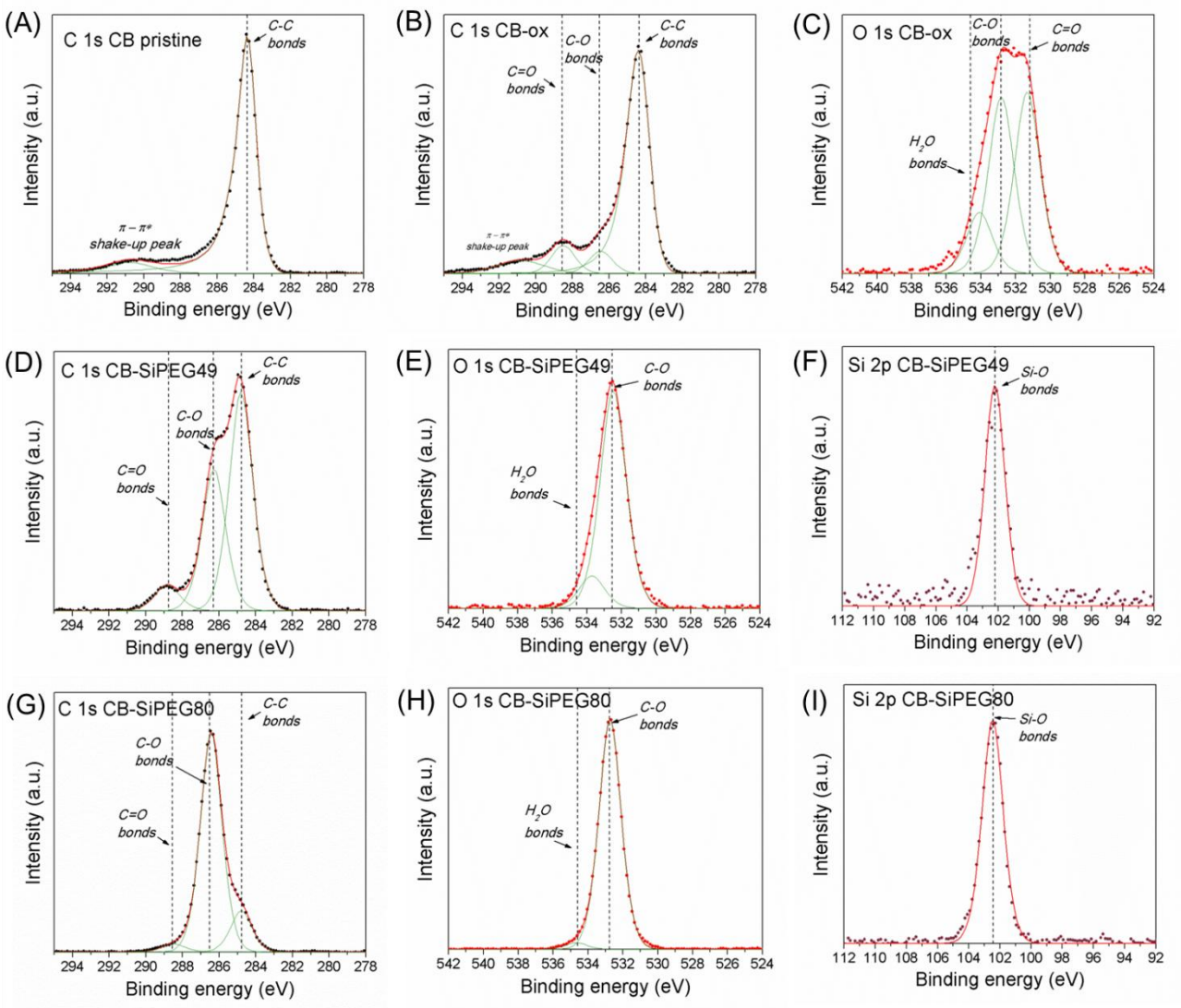


Figure S3. XPS spectra of samples: (A) pristine CB (C 1s); (B, C) CB-ox (C 1s and O 1s); (D-F) CB-SiPEG49 (C 1s, O 1s and Si 2p); (G-I) CB-SiPEG80 (C 1s, O 1s and Si 2p).

Table S1. Components of C 1s XPS spectra of pristine CB, CB-ox and CB-SiPEG samples

Sample	Components from C 1s spectra		
	C-C (%)	C-O (%)	C=O (%)
CB pristine	100	-	-
CB-ox	82	8	10
CB-SiPEG49	56	37	7
CB-SiPEG61	46	50	4
CB-SiPEG71	24	73	3
CB-SiPEG80	15	81	4

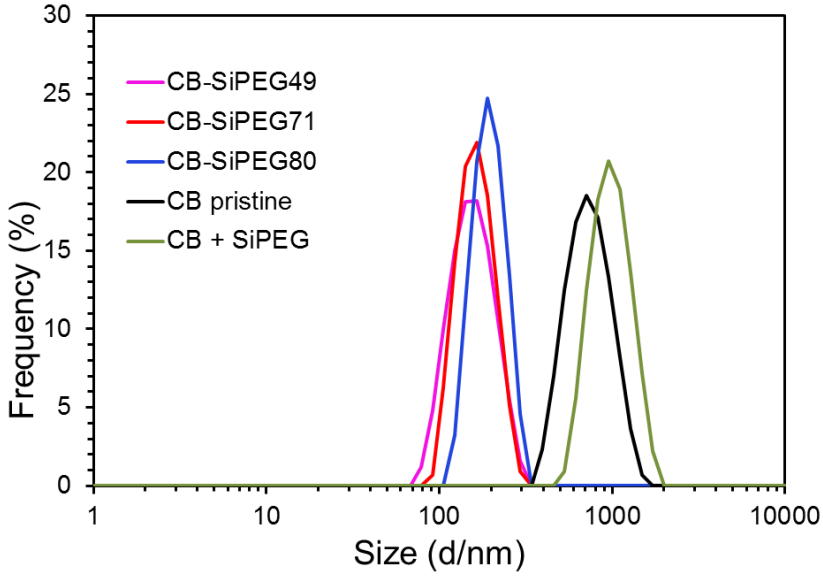


Figure S4. Size distribution of additives dispersed (1% wt.) in PEG200 measured by DLS: pristine CB, CB-SiPEG with three different SiPEG grafting ratios (49, 71 and 80%) and a mixture of CB and free SiPEG (50:50). Temperature: 25ºC.

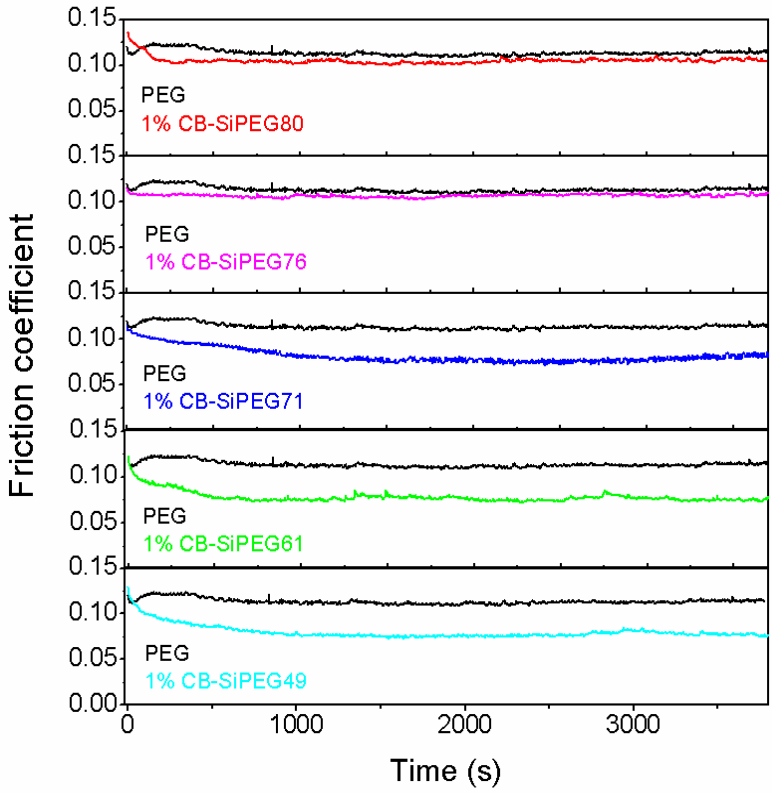


Figure S5. Friction coefficients of 100Cr6 steel sliding surfaces lubricated with neat PEG200 and blends containing 1% wt. CB-SiPEG with different SiPEG grafting ratios. Tribology test parameters: 100Cr6 steel ball and disk, 10 N load, 4 cm s^{-1} sliding speed, 160 m sliding distance and 25ºC temperature.

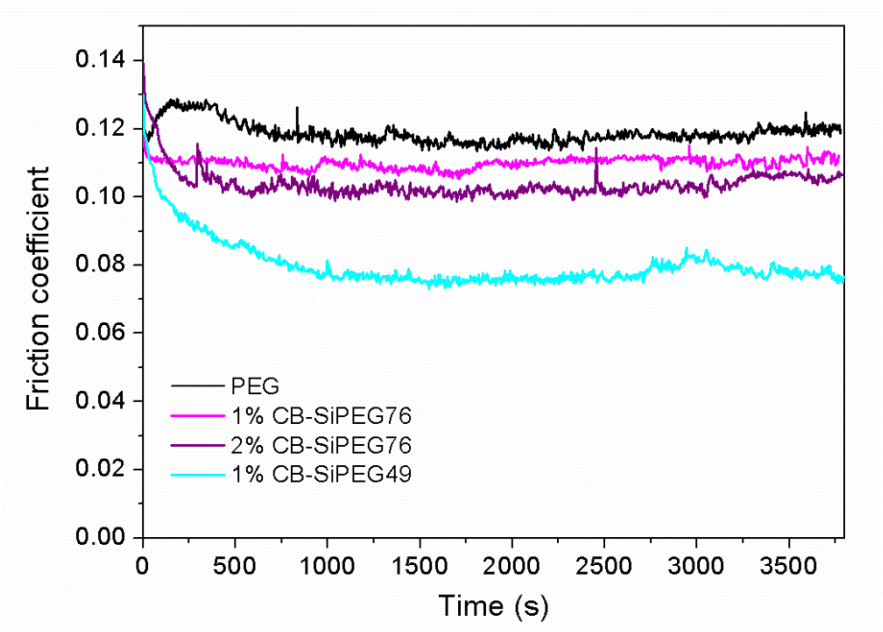


Figure S6. Friction coefficients of 100Cr6 steel sliding surfaces lubricated with neat PEG200 and the following blends: 1% CB-SiPEG49/PEG200, 1% and 2% CB-SiPEG76/PEG200.

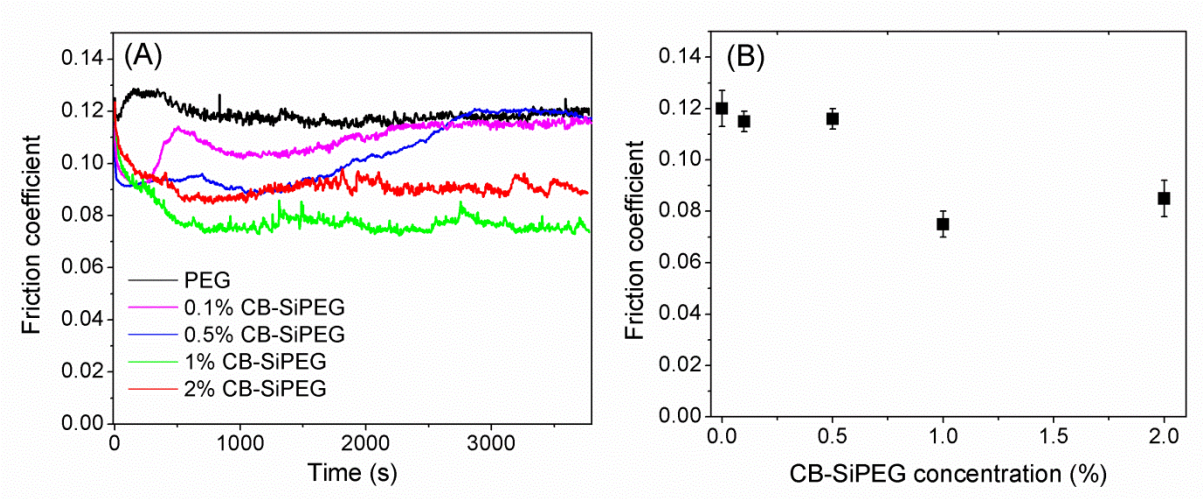


Figure S7. (A) Friction coefficients vs. time of 100Cr6 steel sliding surfaces lubricated with neat PEG200 and blends containing different concentrations of CB-SiPEG61. (B) Average steady-state friction coefficient values with standard deviation for tests run at each CB-SiPEG61 concentration.